Journal of Non-Crystalline Solids 521 (2019) 119497

Contents lists available at ScienceDirect

Journal of Non-Crystalline Solids

journal homepage: www.elsevier.com/locate/jnoncrysol

Low-temperature sintering and densification kinetics of sol-gel derived lithium-mica glass-ceramics through MgF_2 addition

Mohammad Reza Tohidifar*

Department of Materials Science and Engineering, Faculty of Engineering, University of Zanjan, P.O. Box 45371, 38791 Zanjan, Iran

ARTICLE INFO

Keywords:
Densification
MgF_2
Mica glass-ceramic
Sintering
Sol-gel

ABSTRACT

The aim of the current research is to investigate the low-temperature sintering of a nano-crystalline lithium-mica glass-ceramic. Sol-gel technique was used to prepare the glass-ceramics by application of $LiMg_3AlSi_{3(1+x)}O_{10+6x}F_2$ with various x values (0.25, 0.5, 0.75, and 1) and different amounts of MgF_2 as the sintering aid. Use of appropriate amounts of additive and stoichiometric deviation (x) decreased the sintering temperature to 750 °C. Results also revealed that the highest relative density was achieved by applying the optimal amount of additive (4 wt%) with x = 1. The densification activation energy for the glass-ceramic containing 4 wt% MgF_2 was calculated as 214.33 ± 17 kJ mol^{-1}; it was lower than the sample containing 5 wt% additive; hence it was confirmed as optimal content. Consequently, considering densification and phase analysis, true optimum amounts of MgF_2 were determined as 4, 4, 3 and 1 wt% for the glass-ceramics synthesized with x = 1, 0.75, 0.5 and 0.25, respectively.

1. Introduction

Recently, a novel mica glass-ceramic was successfully prepared in which the separated micas are lithium-mica type with lithium ion interlayer cation [1,2]. The potential applications of lithium- mica glass-ceramics have gone beyond their use as machinable ceramics and optical materials; indeed, they are practically applied as lithium ion conductors, heat resistances and electrical insulators in numerous fields [1–5].

The lithium-mica glass-ceramic was first developed by employing the conventional melt-quenching technique using $Li_{(1+x)}Mg_3AlSi_{3(1+x)}O_{10+6.5x}F_2$ composition [1,2]. Although more recent studies have developed new processes using a melt-quenching technique (i.e. precisely controllable fabrication of optical fiber lasers) [6,7], however, forming the glass-ceramic bodies by the melt casting technique is not applicable particularly when it has a complex form. At such conditions, powder-based forming techniques such as pressing, extrusion and sintering the shaped body are recommended. On the other hand, it has been found that the melt-quenching method suffers from some disadvantages such as improper homogeneity, lower purity and higher stoichiometric losses; therefore, sol-gel approach has been strongly recommended [8–14]. Improved homogeneity is vital for the mica glass-ceramics due to presence of the interlocked and randomly-oriented mica crystals with uniform microstructure which provides machinability and good strength of the glass-ceramic. Furthermore, previous works [15–19] were widely focused on sol-gel synthesis of lithium-mica glass-ceramics and optimization of their processes.

Study of the low temperature sintering of the sol-gel lithium-mica glass-ceramic is of crucial importance. As demonstrated before [15], lithium-mica has an unstable phase and transforms to undesirable phases at higher temperatures (> 750 °C). Thus, decreasing the sintering temperature during its production is essential. The viscous flow mechanism is the major approach for densification of glass-ceramics during sintering process. Additionally, some practical techniques including use of materials with finer particle size, chemical process or doping of sintering aid additive can be employed as minor approaches to reduce the sintering temperature [20–23]. The latter technique can be used as an auxiliary mechanism to efficiently improve the glass-ceramics densification. In this method, the glass structure is modified to reduce the viscosity. In the meantime, the simple handling process, lower cost and shorter time are among the advantages of this approach.

In the present research, low temperature sintering of sol-gel derived lithium-mica glass-ceramic was investigated through use of $LiMg_3AlSi_{3(1+x)}O_{10+6x}F_2$ by MgF_2 addition; since some published researches [15,18,19,24] have reported significant improving influence of MgF_2 on the characteristics of mica glass-ceramics. The effects of sintering aid content and stoichiometric deviation from mica composition (x) on the sintering behavior, structural phase analysis and

* Corresponding author.
E-mail address: tohidifar@znu.ac.ir.

https://doi.org/10.1016/j.jnoncrysol.2019.119497
Received 27 January 2019; Received in revised form 4 June 2019; Accepted 5 June 2019
Available online 13 June 2019
0022-3093/ © 2019 Elsevier B.V. All rights reserved.

densification kinetics were also addressed. Differential scanning calorimetry, scanning electron microscopy, x-ray diffraction, three-point bending strength and Archimedean technique were used for characterization of the as-synthesized specimens.

2. Experimental procedure

The lithium-mica glass-ceramics were synthesized using reagent-grade tetraethyl orthosilicate (TEOS; purity ≥99%), aluminum isopropoxide (AIP; purity ≥98%), lithium nitrate (purity ≥98%), magnesium nitrate hexahydrate (purity ≥99%) and ammonium fluoride (purity ≥98%). MgF_2 powder of high purity (99.99%) was also used as sintering aid. Ethyl alcohol (purity ≥99.9%) and toluene (purity ≥99.9%) were employed as chemical solvents while nitric acid (purity ≥65%) was used to control the pH. All the mentioned reagents were supplied from Merck Company (Merck KGaA, Darmstadt, Germany).

The chemicals were measured according to the composition of $LiMg_3AlSi_{3(1+x)}O_{10+6x}F_2$ (x = 0.25, 0.5, 0.75 and 1). First, the calculated amount of $Mg(NO_3)_2.6H_2O$ and $LiNO_3$ was dissolved in ethyl alcohol at pH value of 3–4 (solution A). Specified quantity of AIP was then dissolved in toluene under stirring and named as solution B. The solution C was also provided from specified amount of NH_4F and distilled water whose pH was set at 1–2. Solution A was stirred for 1 h, then, solution B was added to it drop wise under continuous stirring. 30 min later, when the mixed solution became transparent, the pre-hydrolyzed TEOS (for about 30 min; with the molar ratio of TEOS: distilled water: HNO_3 of 1:4:0.05) was added to it (solution A + B) and stirred for 10 min. Finally, the solution C was added drop wise to the above solution and the resulting homogeneous transparent solution was then stirred for about 4 h (the pH of the system ranged in 2–3). The prepared sol was poured into a glass beaker covered with aluminum foil and kept at room temperature until reaching to a gel. The wet gel was then transferred to an oven set at 300 °C for 12 h to evaporate the remaining solvents and burn out the residual organic compositions.

A specified content of dried gel along with 0, 1, 2, 3, 4 and 5 wt% MgF_2 (sintering aid) was ball-milled with ethanol for 6 h. The acquired mixture was again transferred to an oven and heated at 110 °C for 48 h.

The dried glass-ceramic powders were sieved through # 200 mesh and uniaxially pressed under a pressure of 400 MPa for holding time of 5 min to provide a pellet with diameter and thickness of 32 ± 0.5 mm and 3 ± 0.5 mm, respectively. The green compacted products were heat treated at 700 °C for 4 h to crystallize the mica phase and then sintered at ~ 750 °C in a box furnace with the heating rate of 10 °C/min for different periods of time (0.5, 1, 2, 3 and 4 h).

A geometrically approach was employed to determine the green density of the pellets. Bulk density of the fired glass-ceramics was measured by Archimedes method using distilled water. The densification behavior (defined as the ratio of measured bulk densities to the theoretical densities) was also evaluated by assessing relative density of the glass-ceramics. Meanwhile, the theoretical density of the glass-ceramics was measured using helium pycnometer (Micromeritics, AccuPyc II 1340 Norcross, USA).

The sintered glass-ceramics were ground flat using a diamond grinding wheel followed by polishing with finer diamond pastes. The flexural strength was measured using a three-point bending method (ASTM C158–02) by means of Instron Universal Testing Machine (1196, UK) at a bending span and cross-head speed of 20 mm and 0.5 mm/min, respectively. The dimension of specimens was 25 ± 1 mm (length) × 2 ± 0.1 mm (width) × 2.5 ± 0.2 mm (height).

Thermal analyses were conducted to determine the crystallization temperature of glass-ceramics. Differential scanning calorimetry (DSC, Netzsch 409C, Germany) was used with putting 30 mg of sample in the alumina crucible at heating rate of 10 °C/min under an Ar atmosphere with a gas flow rate of 50 mL min^{-1} in temperature range of 25–1000 °C.

The Morphology and microstructure of the sintered glass-ceramics were investigated by employing TESCAN FE-SEM MIRAII scanning electron microscope (SEM). For this purpose, the cross-section of glass-ceramics was highly polished by diamond slurry.

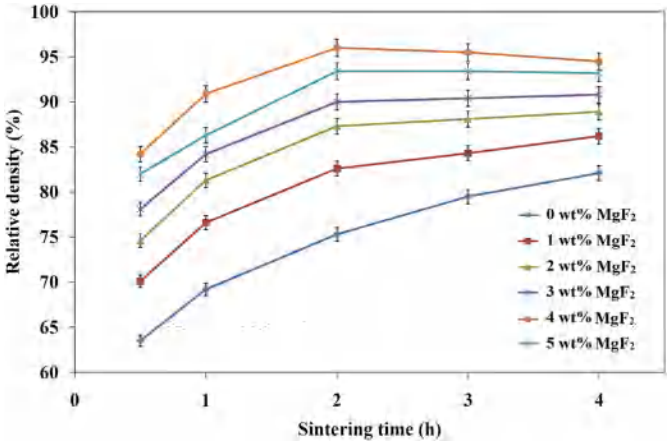

Fig. 1. Sintering time dependence of the relative density of sintered glass-ceramics with stoichiometric deviation of x = 0.5 at 750 °C for various additive contents (uncertainty amounts of all data were estimated 1%).

Phase structures of the sintered glass-ceramics were analyzed by X-ray diffraction (XRD, Philips X'Pert MPD, Netherland) using Co Kα radiation (λ = 1.78897°A) with 2 Theta scan range of 5–80° and step size of 0.02°S^{-1} (operated at 40 kV and 30 mA). The crystalline phase volume fraction of the specimens (I_C) was roughly examined by determining the ratio of the crystalline area (A_C) of the sample's XRD peaks to that of the total area (A_T = crystalline + amorphous) of the same XRD pattern according to the following formula [25]:

$$I_C = \left(\frac{A_C}{A_T}\right) \times 100 \quad (1)$$

3. Results and discussion

Fig. 1 illustrates the dependence of relative density of the glass-ceramics (sintered at 750 °C) on sintering time at the presence of different MgF_2 contents (prepared through stoichiometric deviation of x = 0.5). Densification of the glass-ceramics exhibited an initial rapid increase by enhancement of the sintering time due to completion of diffusion kinetics. It then increased slowly until a constant relative density. Moreover, increase of the MgF_2 content resulted in higher relative density which can be attributed to MgF_2 dissolution into the glass lattice so that non-bridging F sites may depolymerize the glass network. Furthermore, modification of the residual glass structure decreased the viscosity of glass-ceramic [26–30]. Generally, fluorine is a network modifying substance in such a way that two fluorine atoms replace one oxygen atom between abutting tetrahedral without any bond between the fluorine atoms. This phenomenon leads to glass depolymerization [26–30] giving rise to decrease of viscosity through densification process. Any increase in additive content will cause a significant decrease in viscosity of the glass-ceramic through sintering process which is an essential concept in the glass-ceramic densification. Although increase of MgF_2 content led to a glass-ceramic with lower viscosity, increase of the additive content beyond 4% (wt) decreased the relative density since nucleation effect of MgF_2 provided the lithium-mica with more crystallization opportunities.

As demonstrated in previous work [16], MgF_2 particles serve as nucleation center for mica crystallites; hence, the crystallization temperature of the glass-ceramics shifts to lower temperatures. Fig. 2 illustrates the DSC diagram of glass-ceramics synthesized with x = 1 using different amounts of MgF_2. The diagram exhibited an apparent exothermic peak which can be related to the crystallization process. It

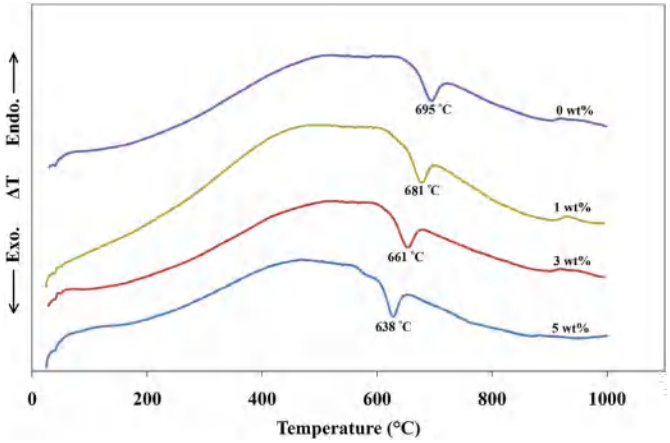

Fig. 2. DSC diagram of lithium-mica glass-ceramics synthesized with different additive contents and x = 1.

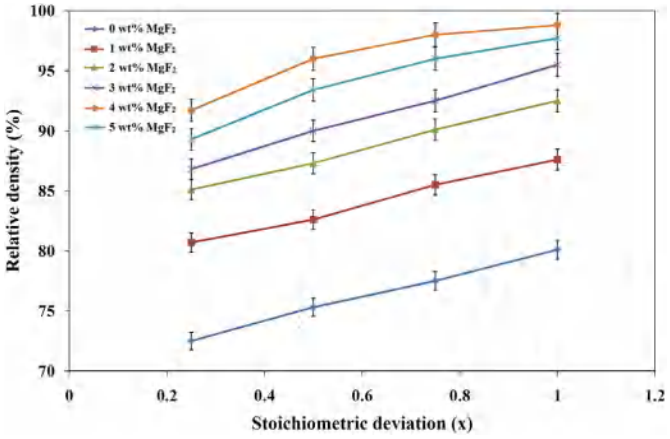

Fig. 3. Stoichiometric deviation (x) dependence of the relative density of glass-ceramics containing different amounts of additive sintered at 750 °C for 2 h (uncertainty amounts of all data were estimated 1%).

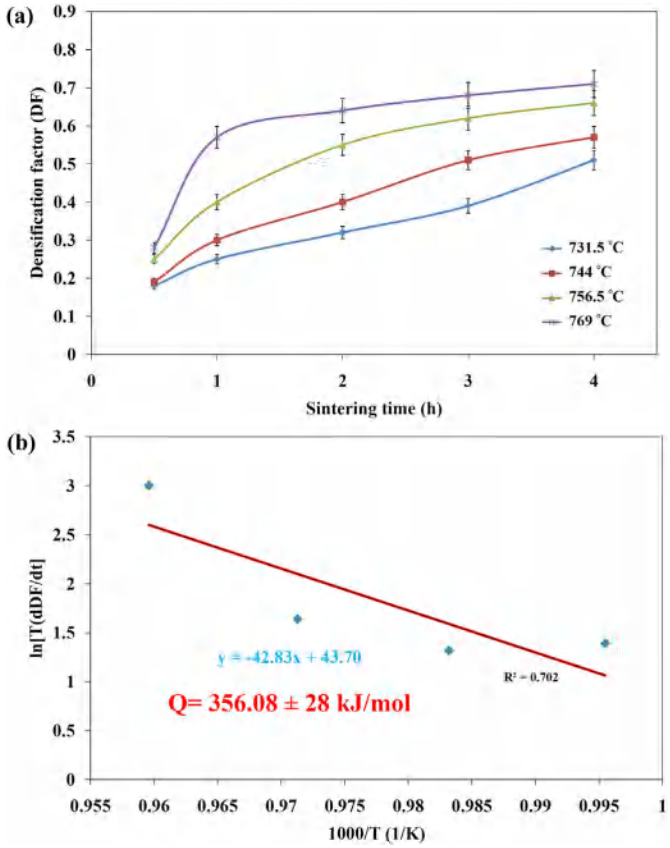

Fig. 4. (a) Densification behavior of the additive-free lithium-mica glass-ceramics sintered at temperatures ranging from 731.5 to 769 °C (uncertainty amounts of all data were estimated 4%) and (b) ln $T\left[\frac{d(DF)}{dt}\right]$ versus 1/T for extracted densification factor based on Fig. 4(a) at DF ranging from 0.4 to 0.5.

was found that crystallization of lithium-mica (JCPDS 025–1388) and other secondary phases i.e. lithium aluminum silicate (JCPDS 040–0073) and forsterite (JCPDS 034–0189) occurred at the same temperature (simultaneous crystallization) [15,16]. It was also concluded that as favored the crystallization conditions in the glass-ceramic, secondary phases will be intensified and lithium-mica gradually attenuated; therefore, the system's crystallinity is too low to be effective in intensifying lithium-mica phase [18,19]. Taking into account the nucleation effect of MgF_2, exothermic peak shifted to lower temperatures by increase of additive content [16]. ΔT = 57 °C was resulted for the transition of exothermic peaks between lower and higher additive amounts so that it confirms the rare crystallization at 700 °C and formation of more amorphous phase [18,19]. In the other words, increase of the exothermic peak temperature (ΔT) along with reduction of the additive content enhanced the crystallization energy at 700 °C. At such conditions, crystallization process retarded giving rise to substantial increase of amorphous phase [18,19]. Thus, decrease of additive content reduced the crystallinity of the glass-ceramic and crystallization of the glass-ceramic was achieved before sintering process, as the crystallization temperature (700 °C) is lower than the sintering temperature (750 °C). Generally speaking, reduction in crystallinity will decrease the viscosity of glass and viscous flow of the residual glass phase is in favor of sintering process [31–33].

It appears that at lower additive contents (≤ 4 wt%), the nucleation behavior of MgF_2 had a poor influence on the relative density compared to its strong impact on viscosity reduction. In contrast, increase in the viscosity (due to increase in crystallization tendency) served as a controlling agent in decrease of densification at higher additive concentrations (> 4 wt%). Therefore, the glass-ceramic containing optimum MgF_2 content (4 wt%) showed the maximum relative density.

As observed, the soaking time of 2 h was considered as the optimum sintering time for the sample with 4 wt% additive since densification rate showed a slight variation and stopped due to grain growth phenomenon. For the samples containing small amounts of additive, however, this phenomenon (over sintering) shifted to the longer times as reduction of the glass-ceramic viscosity was insignificant and viscous flow densification will be completed at higher soaking times.

Fig. 3 shows the variation in the relative density of glass-ceramics sintered at 750 °C for 2 h as a function of their stoichiometric deviation (x). It can be observed that increase of stoichiometric deviation (x) enhanced the relative density of the glass-ceramics in all additive concentrations which can be assigned to substantial formation of the amorphous phase due to increase of x value. Obviously, any increase in the stoichiometric deviation (in $LiMg_3AlSi_{3(1+x)}O_{10+6x}F_2$ composition) gave rise to formation of SiO_2 component. As confirmed in the previous work [18], increase of SiO_2 component (x) could elevate the viscosity of glass-ceramic during crystallization process in a way that it hardly crystallized at its crystallization temperature (700 °C). Thus, a reduction occurred in the crystallinity of the glass-ceramic by increase of x value.

As the glass-ceramic crystallized before sintering process, reduced crystallinity will decrease the viscosity of the glass; therefore, viscous flow of the residual glass will be improved during sintering progress [31–33]. However, the viscous flow of residual glass phase is necessary for glass-ceramic densification so that the glass-ceramic will be

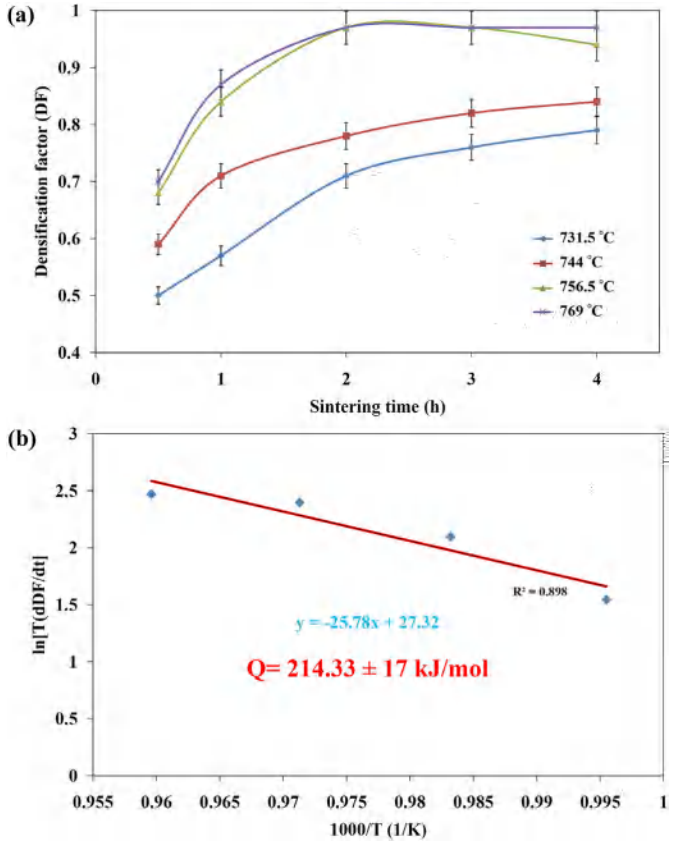

Fig. 5. (a) Densification behavior of lithium-mica glass-ceramics containing 4 wt% additive sintered at temperatures ranging from 731.5 to 769 °C (uncertainty amounts of all data were estimated 4%) and (b) $\ln T\left[\frac{d(DF)}{dt}\right]$ versus 1/T for extracted densification factor based on Fig. 5(a) at DF = 0.7.

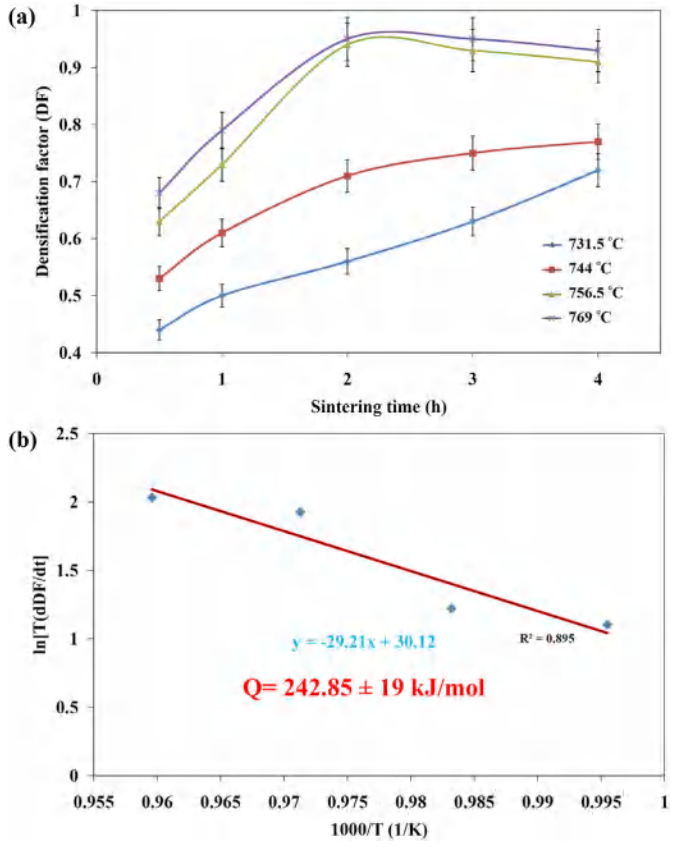

Fig. 6. (a) Densification behavior for the lithium-mica glass-ceramics containing 5 wt% additive sintered at temperatures ranging from 731.5 to 769 °C (uncertainty amounts of all data were estimated 4%) and (b) $\ln T\left[\frac{d(DF)}{dt}\right]$ versus 1/T for extracted densification factor based on Fig. 6(a) at DF = 0.7.

compulsorily densified at lower x values; owing to its widespread crystallization.

As Fig. 3 suggests, at a constant x value, relative density increased by elevating the MgF_2 content (up to 4 wt%). This trend can be attributed to dissolution of MgF_2 into the glass network which may modify the glass structure and decrease the viscosity of glass-ceramic [26–30]. Meanwhile, any increase in additive content dramatically decreased the viscosity of glass-ceramic and therefore a viscous flow may be progressed during sintering process. Incorporation of MgF_2 in the glass-ceramic composition may promote the nucleation effect, since crystallization temperature of the glass-ceramic shifted to the lower temperatures by increase of the additive content (Fig. 2). Densification completion can be indicated from the competition between the viscosity reduction and nucleation effect of the applied additive. For additive concentrations over 4 wt%, contribution of nucleation phenomenon is the dominant mechanism compared to the viscosity reduction; whereas, the effect of MgF_2 presence in reduction of the viscosity was more profound in the glass-ceramics containing < 4 wt% additive. Accordingly, the highest relative density (98.8%) was recorded for the sample containing the optimal amount of MgF_2 (4 wt%) through stoichiometric deviation of x = 1.

In order to consider the densification kinetics and use a thermodynamic approach to confirm the optimum amount of additive, densification factor (DF) which is a function of sintering time was calculated using the following equation [34]:

$$DF = \frac{D_t - D_g}{D_{th} - D_g} \tag{2}$$

In which D_t, D_g and D_{th} are the density of sintered body at time of t, green density and theoretical density, respectively. The densification behavior of several lithium-mica glass-ceramics containing 0, 4 and 5 wt% additive (MgF_2) was calculated at sintering temperatures ranging from 731.5 to 769 °C to evaluate the densification activation energy. Variation of the densification factor was plotted as a function of sintering time in Fig. 4(a) for additive-free glass-ceramics (synthesized with x = 1) sintered at different temperatures. The results showed that densification factors of the glass-ceramics increased by enhancement of the sintering time which could be assigned to faster diffusion kinetics. However, rapid growth of DF values could be observed at the shorter times whereas incremental trend of DF slowly reached to a constant value in prolonged sintering times. In addition, for a constant sintering time, increase of the sintering temperature provided higher densification factor which could be due to porosity removal at elevated temperatures.

Considering DF variations versus sintering time, kinetic analysis of densification was evaluated based on the model proposed by Kingery et al. [35,36]:

$$T\left[\frac{d(DF)}{dt}\right] = K_0 \exp\left(\frac{-Q}{RT}\right) \tag{3}$$

where, DF, K_0, Q, R and T are densification factor, pre-exponential term, densification activation energy, gas constant and absolute temperature, respectively. The above equation can be rewritten as:

$$\ln\left[T\left(\frac{d(DF)}{dt}\right)\right] = \ln K_0 - \frac{Q}{RT} \tag{4}$$

The densification activation energy (Q) can be calculated by plotting $\ln\left[T\left(\frac{d(DF)}{dt}\right)\right]$ versus $1/T$ so that Q can be estimated by the slope of

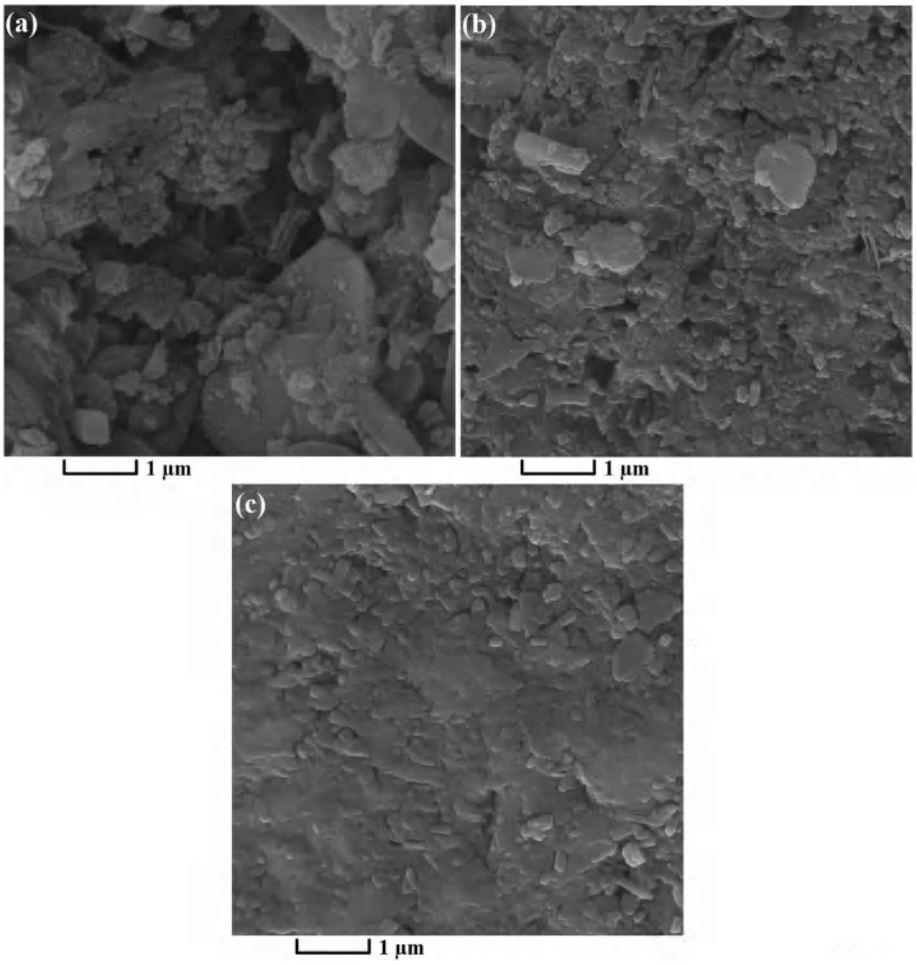

Fig. 7. SEM micrographs of the glass-ceramics sintered at 750 °C for 2 h using. $LiMg_3AlSi_{3(1+x)}O_{10+6x}F_2$ composition with x = 1containing: (a) 0 wt% MgF_2; (b) 5 wt% MgF_2 and (c) 4 wt% MgF_2.

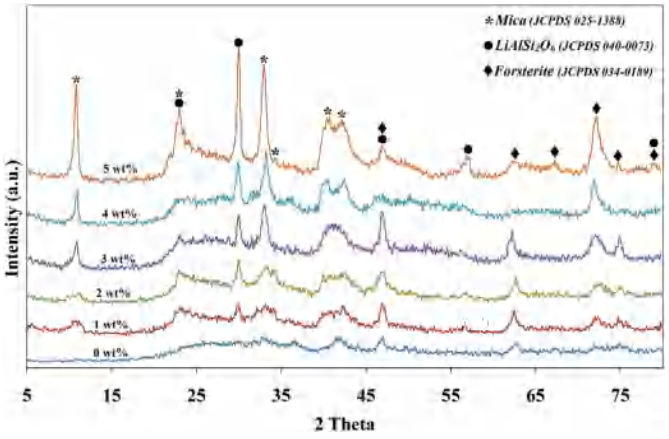

Fig. 8. XRD patterns of the glass-ceramics synthesized with $LiMg_3AlSi_{3(1+x)}O_{10+6x}F_2$ (x = 1) and various MgF_2 contents, sintered at 750 °C for 2 h.

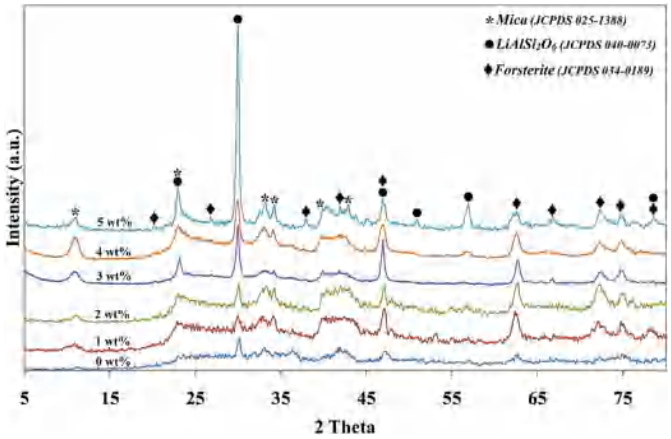

Fig. 9. XRD patterns of the glass-ceramics synthesized with $LiMg_3AlSi_{3(1+x)}O_{10+6x}F_2$ (x = 0.75) and various MgF_2 contents, sintered at 750 °C for 2 h.

the straight line.

Fig. 4(b) shows the Arrhenius plots of $\ln\left[T\left(\frac{d(DF)}{dt}\right)\right]$ versus $1/T$ based on the densification data extracted from Fig. 4(a) at DF values ranging from 0.4 to 0.5. Least squares fit method was employed for regression analysis and determination of the slope of straight line. The aforementioned densification activation energy for additive-free lithium-mica glass-ceramics (synthesized with x = 1) was determined as 356.08 ± 28 kJ mol^{-1}.

The densification activation energy of the glass-ceramics containing 4 and 5 wt% MgF_2 were also calculated as 214.33 ± 17 and 242.85 ± 19 kJ mol^{-1} according to Fig. 5 and Fig. 6, respectively. Clearly, the sample containing 4 wt% MgF_2 exhibited lower activation energy compared to the additive-free one. This highlights the sintering aid behavior of MgF_2 as it provided a thermodynamically favorable

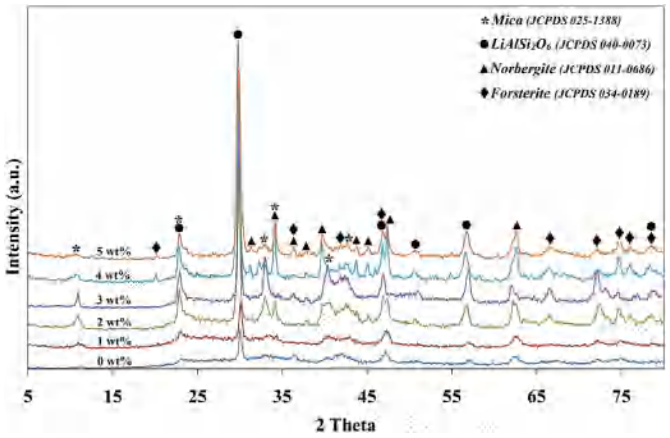

Fig. 10. XRD patterns of the glass-ceramics synthesized with $LiMg_3AlSi_{3(1+x)}O_{10+6x}F_2$ (x = 0.5) and various MgF_2 contents, sintered at 750 °C for 2 h.

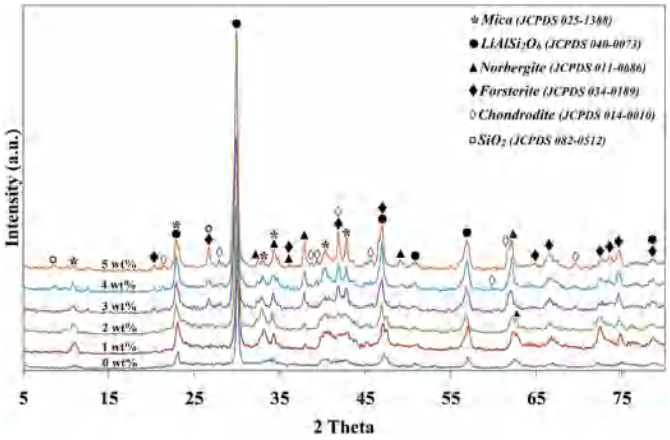

Fig. 11. XRD patterns of the glass-ceramics synthesized with $LiMg_3AlSi_{3(1+x)}O_{10+6x}F_2$ (x = 0.25) and various MgF_2 contents, sintered at 750 °C for 2 h.

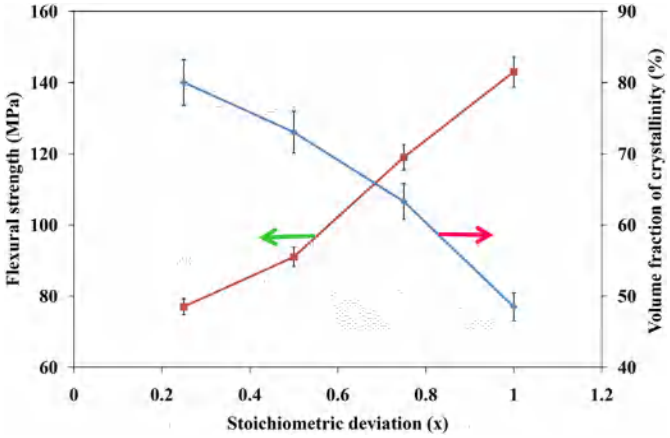

Fig. 12. Variations of the flexural strength and crystalline phase volume of the glass-ceramics by stoichiometric deviation (x) for specimen containing 4 wt% sintering aid (uncertainty amounts of all data were estimated 3 and 4%, respectively).

condition to achieve the densification process. This can be attributed to additive dissolution in glass structure and reduced viscosity as discussed in previous section. Moreover, densification activation energy of the glass-ceramic prepared with 5 wt% MgF_2 was higher than that of the sample containing 4 wt% MgF_2 which confirmed the difficulty of porosity elimination in the glass-ceramic containing 5 wt% MgF_2. As mentioned earlier, nucleation behavior of MgF_2 enhanced by increase of additive content; hence, nucleation effect-induced crystallization was anticipated to reduce the viscosity of the glass-ceramic containing 5 wt % MgF_2. This verifies 4 wt% MgF_2 as the optimal content of sintering aid.

Fig. 7 shows the SEM micrographs of the glass-ceramics sintered at 750 °C for 2 h with different amounts of sintering aid using $LiMg_3AlSi_{3(1+x)}O_{10+6x}F_2$ composition with x = 1. The cross-section of the glass-ceramics was highly polished so that the glassy phase could be identified; this was possible without chemically etching in the back-scattered contrast. The images revealed that densification of the samples having 0 and 5 wt% MgF_2 (Fig. 7(a) and Fig. 7(b)) was imperfect since the residual glass had higher viscosity than what was required to fully rearrange of the particles. Fig. 7(c) shows the sample in which sintering aid content is at its optimum value (4 wt%). In such condition, the glassy phase was able to fully penetrate the grains to form a thin layer that separated the grains from each other; thus, this promoted densification by controlling the challenge of viscous flow against nucleation effect of MgF_2. This sample possessed the highest relative density of 98.8%.

Fig. 8 shows the XRD patterns of the glass-ceramics synthesized through the composition $LiMg_3AlSi_{3(1+x)}O_{10+6x}F_2$ (x = 1) with different MgF_2 contents sintered at 750 °C for 2 h. It can be observed that crystallinity of glass-ceramics increased by increment of MgF_2 content. As demonstrated before [18], the viscosity of the glass-ceramic with x = 1was higher as it encompassed higher levels of SiO_2. In such condition, the crystallization temperature of the glass-ceramic showed a shift to higher temperatures giving rise to a reduction in the system crystallinity. On the other hand, the presence of MgF_2 can directly decline the viscosity of the glass-ceramic during crystallization process and consequently, increase the system crystallinity. As shown in Fig. 8, any increase in the amount of additive (x = 1) resulted in more profound lithium-mica phase (JCPDS 025–1388) which can be assigned to nucleation performance of the additive. The amorphous character of the glass-ceramic prepared with x = 1 was too high; in a way that increase of additive content up to 5 wt% could not further enhance the crystallization of secondary phases. Therefore, the presence of additive in the glass-ceramic with x = 1, not only promoted the crystallization process but also improved the mica peak intensity.

Fig. 9 depicts the diffractogram of the specimens fabricated with $LiMg_3AlSi_{3(1+x)}O_{10+6x}F_2$ composition (x = 0.75) with different additive contents after 2 h of sintering at 750 °C. On general, the glass-ceramics prepared with x = 0.75 had higher crystallinity compared to those with x = 1. Based on Fig. 3, more incorporation of additive can be helpful in decreasing the crystallization temperature and encourages the formation of secondary phases i.e. lithium aluminum silicate (JCPDS 040–0073). Weak mica peaks could also emerge. It appears that 4 wt% is the optimal additive content to intensify mica phase for x = 0.75.

Fig. 10 and Fig. 11 show the XRD patterns of the glass-ceramics synthesized with x = 0.5 and x = 0.25 at different MgF_2 contents after 2 h of sintering at 750 °C, respectively. Formation of high intensity peaks could be assigned to formation of undesirable phases which can be easily observed in the glass-ceramics at low x values (0.25 and 0.5). Presence of sintering aid additive can increase the system crystallinity (owing to its nucleation role); so, the level of MgF_2 should be decreased to prevent from further crystallization. This can intensify the secondary phases and attenuate mica intensity. Therefore, the maximum amount of additives giving rise to higher intensity of lithium mica peak was determined as 3 and 1 wt% for the glass-ceramics prepared with x = 0.5 and 0.25, respectively.

Although the apparent optimum additive content leading to a glass-ceramic with higher relative density was 4 wt%, based on structural phase analysis, the true optimum amounts of additive were however

determined as 5, 4, 3 and 1 wt% for the samples prepared with x = 1, 0.75, 0.5 and 0.25, respectively. Regarding the intersection of the optimum amount ranges, the true optimum content of the sintering aid was determined as 4, 4, 3 and 1 wt% for the glass-ceramics synthesized with x = 1, 0.75, 0.5 and 0.25, respectively.

As shown above, the apparent optimal concentration of additive was 4 wt% as it resulted in the lowest activation energy. However, according to the XRD patterns in Fig. 11, the transformation and formation of new phases were accompanied by the energy gain and loss. Therefore, the difference in activation energy of two samples may be considered as crystallization energy required for developing the new phases. It can be supposed that 113.23 kJ mol^{-1} is the approximated required energy for crystallization of some minor phases i.e. Chondrodite (JCPDS 014–0010), Norbergite (JCPDS 011–0686) and SiO_2 (JCPDS 082–0512) which was calculated from the activation energy of the samples containing 0 and 5 wt% MgF_2.

Variations of the flexural strength and crystalline phase volume of the glass-ceramics (sintered at 750 °C for 2 h) by their stoichiometric deviation (x) are plotted in Fig. 12 for the case with 4 wt% sintering aid. Although the flexural strength increased at higher x values, the crystalline phase volume showed a drastic decline. It is obvious that the viscous flow mechanism was considerably activated by increase of x value (reduction in crystallization volume) so that a poor crystallization decreased the viscosity of glass and promoted the viscous flow of residual glass. At the same time, incorporation of an optimum additive content (4 wt%) resulted in proper viscosity, which increased the densification rate and removed the porosities; giving rise to an increase in flexural strength.

4. Conclusion

The present study developed a lithium-mica glass-ceramic for sintering at lower temperatures. Following conclusions can be made:

1. Application of a proper content of sintering aid (MgF_2) in the glass-ceramic resulted in a body with the relative density of 98.8%.
2. In order to achieve high relative density, the sintering temperature was decreased to 750 °C by considering optimal amount of MgF_2 (4 wt%) along with stoichiometric deviation of x = 1.
3. The true optimum amount of sintering aid depended on stoichiometric deviation. 4% (wt) additive content was assessed as true optimal value for glass-ceramics with x = 1 and 0.75; while, this parameter was determined as 3 and 1 wt% for glass-ceramics prepared with x = 0.5 and 0.25, respectively.
4. The densification activation energy for the glass-ceramics containing 0, 4 and 5 wt% of MgF_2 were calculated as 356.08 ± 28, 214.33 ± 17 and 242.85 ± 19 kJ mol^{-1}, respectively; suggesting 4 wt% as the apparent optimal additive content.

References

[1] S. Taruta, T. Ichinose, T. Yamaguchi, K. Kitajima, Preparation of transparent lithium-mica glass-ceramic, J. Non-Cryst. Solids 352 (2006) 5556–5563.
[2] S. Taruta, M. Suzuki, T. Yamakami, T. Yamaguchi, K. Kitajima, Preparation and ionic conductivity of transparent glass-ceramics containing a large quantity of lithium-mica, J. Non-Cryst. Solids 354 (2008) 848–855.
[3] S. Taruta, M. Matsuki, H. Nishikiori, T. Yamakami, T. Yamaguchi, K. Kitajima, Preparation and luminescent properties of Eu-doped transparent mica glass-ceramic, Ceram. Int. 36 (2010) 1303–1309.
[4] A. Faeghi Nia, Thermal properties and crystallization of lithium-mica glass and glass-ceramics, Thermochim. Acta 564 (2013) 1–6.
[5] V. Khani, P. Alizadeh, M.S. Shakeri, Optical properties of transparent glass-ceramics containing lithium-mica nanocrystals: crystallization effect, Mater. Res. Bull. 48 (2013) 3579–3584.
[6] Sh. Kang, Z. Fang, X. Huang, Zh. Chen, D. Yang, X. Xiao, J. Qiu, G. Dong, Precisely controllable fabrication of Er^{3+}-doped glass ceramic fibers: novel mid-infrared fiber laser materials, J. Mater. Chem. C 5 (2017) 4549–4556.
[7] Z. Fang, Sh. Zheng, W. Peng, H. Zhang, Zh. Ma, Sh. Zhou, D. Chen, J. Qiu, Fabrication and characterization of glass-ceramic fiber-containing Cr^{3+}-doped $ZnAl_2O_4$ nanocrystals, J. Am. Ceram. Soc. 98 (9) (2015) 2772–2775.
[8] I. Cacciotti, Bivalent cationic ions doped bioactive glasses: the influence of magnesium, zinc, strontium and copper on the physical and biological properties, J. Mater. Sci. 52 (2017) 8812–8831.
[9] M. Ding, Ch. Lu, L. Chen, W. Bai, Y. Yung, Zh. Ji, Transparent sol-gel glass ceramics containing β-NaYF4:Yb^{3+}/Er^{3+} nanocrystals: structure, upconversion luminescent properties and optical thermometry behavior, Ceram. Int. 44 (2018) 16379–16387.
[10] M. Lombardi, L. Gremillard, J. Chevalier, L. Lefebvre, I. Cscciotti, A. Bianco, L. Montanaro, A comparative study between melt-derived and sol-gel synthesized 45S5 bioactive glasses, Key Eng. Mater. 541 (2013) 15–30.
[11] Ch.L. Huang, W. Fang, I.H. Chen, T.Y. Hung, Manufacture biomimetic mineral deposition of nanoscale bioactive glasses with mesoporous structures using sol-gel methods, Ceram. Int. 44 (2018) 17224–17229.
[12] I. Cacciotti, M. Lombardi, A. Bianco, A. Ravaglioli, L. Montanaro, Sol-gel derived 45S5 bioglass:synthesis, microstructural evolution and thermal behavior, J. Mater. Sci. Mater. Med. 23 (8) (2012) 1849–1866.
[13] M. Ding, J. Hou, Z. Cui, H. Gao, Ch. Lu, J. Xi, Zh. Ji, D. Chen, Bundle-shaped β-$NaYF_4$ microrods: hydrothermal synthesis, Gd-mediated downconversion luminescence and ratiometric temperature sensing, Ceram. Int. 44 (2018) 7930–7938.
[14] M. Lombardi, I. Cacciotti, A. Bianco, L. Montanaro, RKKP bioactive glass-ceramic material through an aqueous sol-gel process, Ceram. Int. 41 (2015) 3371–3380.
[15] M.R. Tohidifar, P. Alizadeh, P. Riello, B. Eftekhari Yekta, A.R. Aghaei, Sol-gel preparation and characterization of nano-crystalline lithium-mica glass-ceramic, Ceram. Int. 38 (2012) 2813–2821.
[16] M.R. Tohidifar, P. Alizadeh, P. Riello, Nucleation and crystallization behaviors of nano-crystalline lithium-mica glass-ceramic prepared via sol-gel method, Mater. Res. Bull. 47 (2012) 1374–1378.
[17] M.R. Tohidifar, P. Alizadeh, A.R. Aghaei, Controlling the sol-gel process of nano-crystalline lithium-mica glass-ceramic by its chemical composition and synthesis parameters, Mater. Charact. 99 (2015) 61–67.
[18] M.R. Tohidifar, P. Alizadeh, Structural phase analysis of a sol-gel nano-crystalline lithium-mica glass-ceramic through different compositions, Mater. Chem. Phys. 179 (2016) 160–165.
[19] M.R. Tohidifar, On the analysis and optimization of lithium-mica nano-crystallites using a statistical technique, Mater. Charact. 127 (2017) 333–341.
[20] H. Wu, Q. Mei, Ch. Xing, J. Bi, Effects of B_2O_3 addition on sintering behavior and microwave dielectric properties of ixiolite-structure $ZnTiNb_2O_8$ ceramics, J. Alloys Compd. 679 (2016) 26–31.
[21] B. Liu, L. Yi, X.M. Chen, Effects of B_2O_3 addition on sintering behavior and microwave dielectric properties of $(Sr_{0.6}Ca_{0.4})LaAlO_4$ ceramics, Mater. Res. Bull. 67 (2015) 230–233.
[22] Y. Song, Q. Sun, Y. Lu, X. Liu, F. Wang, Low-temperature sintering and enhanced thermoelectric properties of $LaCoO_3$ ceramics with B_2O_3-CuO addition, J. Alloys Compd. 536 (2012) 150–154.
[23] K.W. Tay, Y.P. Fu, J.F. Huang, H.Ch. Huang, Effect of Bi_2O_3 and B_2O_3 additives on the sintering temperature, microstructure, and microwave dielectric properties for $Sm(Mg_{0.5}Ti_{0.5})O_3$ ceramics, Ceram. Int. 37 (2011) 1025–1031.
[24] D.P. Mukherjee, A.R. Molla, S.K. Das, The influence of MgF_2 content on the characteristic improvement of machinable glass ceramics, J. Non-Crys. Solids 433 (2016) 51–59.
[25] S. Krimm, A.V. Tobolski, Quantitative X-ray studies of order in amorphous and crystalline polymers. Quantitative X-ray determination of crystallinity in polyethylene, J. Polym. Sci. 7 (1951) 57–76.
[26] A. Baasner, B.C. Schmidt, S.L. Webb, The effect of chlorine, fluorine and water on the viscosity of aluminosilicate melts, Chem. Geol. 357 (2013) 134–149.
[27] A. Bartels, H. Behrens, F. Holtz, B.C. Schmidt, M. Fechtelkord, J. Knipping, L. Crede, A. Baasner, N. Pukallus, The effect of fluorine, boron and phosphorus on the viscosity of pegmatite forming melts, Chem. Geol. 346 (2013) 184–198.
[28] M. Zimova, S.L. Webb, The combined effects of chlorine and fluorine on the viscosity of aluminosilicate melts, Geochim. Cosmochim. Acta 71 (2007) 1553–1562.
[29] K. Stanton, R.J. Hill, The roll of fluorine in the devitrification of SiO_2.Al_2O_3.P_2O_5.CaO.CaF_2 glasses, J. Mater. Sci. 35 (2000) 1911–1916.
[30] C.O. Freeman, I.M. Brooks, A. Johnson, P.V. Hatton, R.G. Hill, K.T. Stanton, Crystallization modifies osteoconductivity in an apatite-mullite glass-ceramic, J. Mater. Sci. Mater. Med. 14 (2003) 985–990.
[31] W. Gong, H. Li, L. Wang, E. Wang, Pressureless sintering and mechanical properties of 3Y-TZP-reinforced LZAS glass-ceramic composites, Ceram. Int. 42 (2016) 18053–18057.
[32] H.I. Hsiang, L.T. Mei, Sh.W. Yang, W.Ch. Liao, F.S. Yen, Effects of alumina on the crystallization behavior, densification and dielectric properties of BaO-ZnO-SrO-CaO-Nd_2O_3-TiO_2-B_2O_3-SiO_2 glass-ceramics, Ceram. Int. 37 (2011) 2453–2458.
[33] A.I. Borhan, M. Gromada, G.G. Nedelcu, L. Leontie, Influence of (CoO,CaO,B_2O_3) additives on thermal and dielectric properties of BaO-Al_2O_3-SiO_2 glass-ceramic sealant for OTM applications, Ceram. Int. 42 (2016) 10459–10468.
[34] J.H. Jean, T.K. Gupta, Densification kinetics and modeling of glass-filled alumina composite, J. Mater. Res. 9 (1994) 771–780.
[35] W.D. Kingery, E. Niki, M.D. Narasimhan, Sintering of oxide and carbide-metal compositions in presence of a liquid phase, J. Am. Ceram. Soc. 44 (1961) 29–35.
[36] J.H. Jean, S.C. Lin, Effects of borosilicate glass on densification and properties of borosilicate glass + TiO_2 ceramics, J. Mater. Res. 14 (1999) 1359–1363.